Shear Yield and Crazing Stresses in Selected Glassy Polymers

RICHARD M. IKEDA

Central Research and Development, Du Pont Experimental Station, Wilmington, Delaware 19880-0356

SYNOPSIS

The plane strain shear yield stress and the triaxial crazing stress were determined for several commercial glassy polymers as a function of temperature. The polymers considered were: polycarbonate (Lexan®), polysulfone (Udel®), polyetherimide (Ultem®), polyarylate (Arylon®), and an amorphous nylon (Zytel® 330). When normalized to T_g the data for the various polymers were similar but not identical. An exception may be the triaxial crazing strains. In the temperature region between $[T - T_g] = -300°$ and $-50°$C the crazing strains were all small (<1.5%), showed little temperature dependence, and appeared identical within the precision of our measurements. For temperatures below T_g and above any major secondary relaxation, Poisson's ratio was found to be constant for all of the polymers examined, 0.42 (±5%). © 1993 John Wiley & Sons, Inc.

INTRODUCTION

In many early polymer applications the dimensions and shapes of the parts were such that the primary mode of response was shear deformation (i.e., shape change) and the useful characterization parameter was the shear yield stress. Plastics were usually considered "tough" since they underwent extensive deformation before breaking. In more recent structural applications such as composites, because of size and construction geometries, polymers are sometimes subjected to triaxial states of stress. From an engineering point of view, this has led to the increasing application of fracture mechanics concepts to polymer solids.[1] From a mechanistic viewpoint, the triaxial forces tending to increase the volume of polymer usually lead to a special type of cavitation–crazing. The crazing stress (or strain) is thus an important characterization parameter for polymers and must be added to the yield stress to describe mechanical failure. The consideration of crazing is not new.[2] In fact, the molecular understanding of crazing probably surpasses our detailed knowledge of yielding.[3] The growing structural applications of polymers merely highlights the addition of crazing parameters in engineering failure computations and predictions.

EXPERIMENTS AND RESULTS

The literature[4] yields a rather limited number of techniques that have been used to determine the yield stress of polymer materials and an even smaller number of experiments to determine the crazing stress. The use of tensile experiments to measure the yield stress is the most common. It suffers from two problems: a new tensile bar must be used for each determinations; and the stress–strain curves frequently do not show an easily recognizable "knee" or maximum and one is forced to use a more arbitrary definition of yield (i.e., 0.2% strain off-set). Walrath and Adams[5] used the Iosipescue shear test method to measure yield stresses in polymers and composite samples. With neat polymers, we found that this measurement frequently did not exhibit an easily recognizable knee and each sample required a bonded strain gauge thus complicating the multiple determination problem. The classical shear experiment involves the twisting of a cylindrical sample.[4] We did not consider these measurements since cylindrical samples are not easily available to us. The technique adopted for this work was a compression

Journal of Applied Polymer Science, Vol. 47, 619–629 (1993)
 CCC 0021-8995/93/040619-11

or indentation test.[6] We found that there was some ambiguity in the analysis of the results but the simplicity of the test, its reproducibility, and its consistency with tensile experiments led us to adopt it for this study.

The literature yields three techniques to measure the crazing stresses in polymers. Gent[7] imbedded spherical inclusions in elastomer samples and carefully noted the far field stresses on the sample when voids were formed near the inclusions. The traction on the sample at the point of cavitation could then be computed. Sample preparation is an obvious problem if this technique were used as a general characterization method. Probably the most highly developed and precise method is that used by Kramer and Berger[3] and others.[8] They statistically determine the crazing strains and use tensile moduli to calculate the crazing stresses. The technique uses thin film samples, deposited from solution, and thus their measurements are usually done under plane stress conditions. We wanted information obtained under plane strain conditions. Information on hand indicates that the crazing stresses are the same under both conditions of stress[9] so this may not be a problem. A possible drawback to the general utility of this technique lies in the equivalence of the solution deposited sample and the bulk materials actually used in the various applications. This could be circumvented by the elliptical bending technique used by Kambour[10] to determine the crazing strain but the general application of this technique to all glassy polymers is difficult. Many will yield and not craze. The third experimental technique involves the breaking of specimens with blunt notches and a determination of the position of the crazes with respect to the notch. One then makes use of the slip line theory developed by Hill[11] to obtain a relationship between the shear yield and crazing stress. This methodology has been used with success by Ishikawa and Narizawa[12] to examine the effects of aging in glassy polymers and was adopted for this study.

Table I Sample Identification

Sample	Source	T_g1	T_g2	Density
Polyarylate	Arylon®	178	...	...
		172	170	1.209
Polysulfone	Udel®	176	175	1.233
Polyetherimide	Ultem®	201	201	1.282
Polycarbonate	Lexan®	...	139	1.199
Amorphous nylon	Zytel® 330	129	134	1.159

T_g1, DSC determination; T_g2, volume/temperature determination. Density, gm/cc (helium pycnometer).

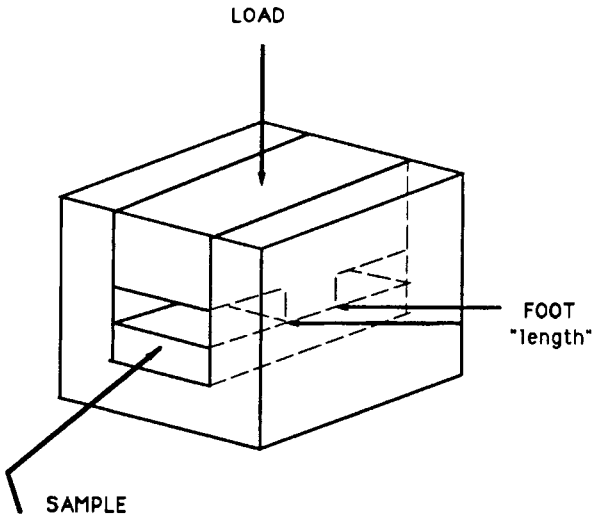

Figure 1 Schematic of compression apparatus.

Test Samples

Samples were collected in the form of $\frac{1}{2}$-in.-wide flex bars. Where possible, bars with $\frac{1}{8}$ and $\frac{1}{4}$ in. thicknesses were also obtained. After notching, all materials were heated to 5–10°C above their T_g for at least $\frac{1}{2}$ h in an oven and the oven turned off and allowed to cool to room temperature overnight using a dry nitrogen atmosphere. Table I lists the samples and T_g information.

Compressional Yield Measurements

One-half-in.-wide tensile bars were compressed while confined in a $\frac{1}{2}$-in. slot as shown in Figure 1.

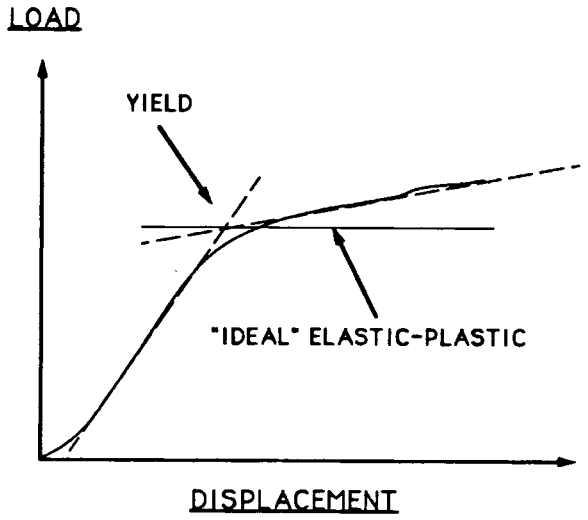

Figure 2 Load-displacement curve. The intersection of the dashed lines are used to determine the load at yield.

Table II Effect of Geometry on Compression Load

Anvil Length (in.)	Sample Length (in.)	Load at Yield (MPa)
0.125	6.000	102 ± 2
0.125	0.125	101 ± 3
0.250	6.000	98 ± 3
0.250	0.250	96 ± 3
0.500	6.000	102 ± 2
0.500	0.500	99 ± 2

The indenter that was finally chosen was $\frac{1}{2}$ in. wide and $\frac{1}{8}$ in. long. A typical load-displacement trace is shown in Figure 2. In all cases an easily recognizable knee was exhibited. Figure 2 also contains a graphical description of the method used to determine the load at yield. Using polycarbonate samples, trial experiments were made with, and without, Nujol® lubricant using indenters of $\frac{1}{8}''$, $\frac{1}{4}''$ and $\frac{1}{2}''$ length. Different sample lengths were also used [very long (6″) and equivalent to the indenter lengths]. As long as the lubricant was used, the data were quite consistent as shown in Table II.

Elastic-Plastic Assumption and Slip Line Theory of Hill[11]

To convert the measured load into a useful material characteristic we must make some assumptions about the nature of glassy polymers. We chose to characterize them as ideal elastic-plastic materials.[11] Below T_g our glassy polymers exhibited localized yielding, slip lines, and their load-displacement curves resemble the two straight lines of an ideally elastic-plastic material (Fig. 2). A correction to the measured loads is necessitated by the fact that the indentations were made on samples of finite thickness. The correction factors have been computed by Hill.[10] Since we used samples of two different thicknesses, a simple consistency check can be made. The results are shown in Table III. The internal checks are quite good.

The Effect of Strain Rate

The effect of strain rate on the yield stress is a well known and documented phenomenon.[13–15] The compression determinations behave similarly as shown in Figure 3 where we compare compression and tensile data for polyarylate samples at 25°C and comparable strain rates. The rate dependence is 4 MPa per decade. In all subsequent experiments the compression strain rate was either 1 or 2×10^{-3} (1/sec).

Assumption of Von Mises Yield Criterion[11]

To compare our compression yield stresses those determined by other means, we have assumed a Von Mises yield criterion to obtain the expression (Appendix A):

$$Y = S\sqrt{(1 - \nu + \nu^2)}. \qquad (1)$$

Here Y is the tensile yield stress, S our compressional yield stress, and ν Poisson's ratio. To a good approximation one can assume 0.42 for Poisson's ratio and not introduce serious error (below).

Comparisons with Literature Data

In Figures 4–8 are displayed tensile yield data computed from our compression experiments using eq. (1). Each open circle represents the average of 8–10 replicate measurements. To a fair approximation, the semilog plots of the yield stresses versus temperature are linear. In four of the five figures, literature tensile data are also plotted. In most cases the strain rates were fairly comparable (i.e., within a factor of 50) and the differences should not result in major shifts of the data.

Table III Correction for Sample Thickness

		Yield Stress (MPa)			
		Measured		Corrected	
Sample	t (C)	0.125″	0.250″	0.125″	0.250″
Arylon®	−25	143.7 ± 3.0	195.0 ± 5.0	118.8 ± 2.5	114.0 ± 3.0
	0	122.5 ± 1.5	173.8 ± 2.1	101.2 ± 1.2	101.6 ± 1.2
	100	68.9 ± 1.9	86.6 ± 3.0	56.9 ± 1.6	50.6 ± 2.0
Udel®	75	79.2 ± 1.9	108.6 ± 4.0	65.4 ± 1.6	63.5 ± 2.3

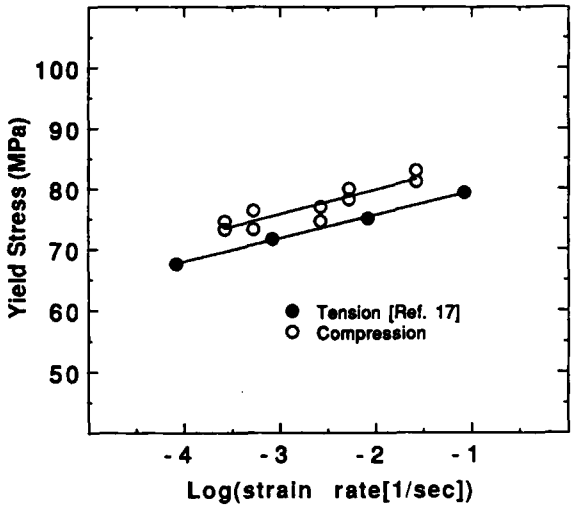

Figure 3 Effect of strain rate on the yield stress. The test samples were polyarylate (Arylon®).

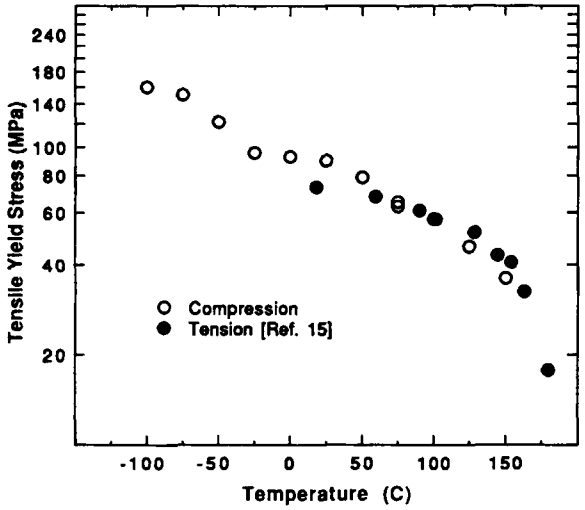

Figure 5 Tensile yield stresses for Udel®. The open circles were computed from compression data.

Except for the Zytel® 330 data, the comparisons between our compression data and literature tensile data are quite good, especially at the higher temperatures. At the lower temperatures the tensile data tend to be lower. This would be quite reasonable if there is a pressure dependence of the yield stress.

For Zytel® 330 the situation is different. The tensile data are actually stress at break information. Since the elongation at break is substantial (ca. 100%), we must assume that the tensile data represent an upper bound to the tensile yield stress and our discrepancy may be more than it appears. If the comparison is valid, the pressure dependence of the critical yield stress might be unusually high (see following) or the moisture contents might be different. We took care to keep our samples dry but we have no information on the moisture content of the samples used in the tensile test. A higher moisture content would also lead to lower yield values.

Another test of our data can be obtained by comparison with the plane stress yield strain data of Plummer and Donald.[9] This is shown in Figure 9 where we have used Poisson's ratio information and Young's modulus data to convert our compression yield stress data to tensile yield strains. The temperature dependence of both sets of data are very

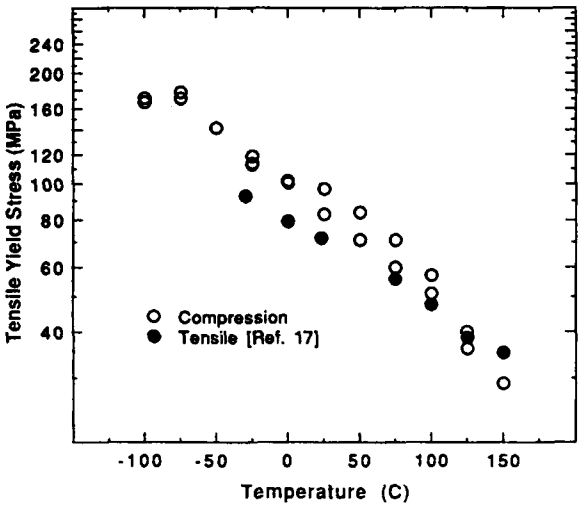

Figure 4 Tensile yield stresses for Arylon®. The open circles were computed from compression data.

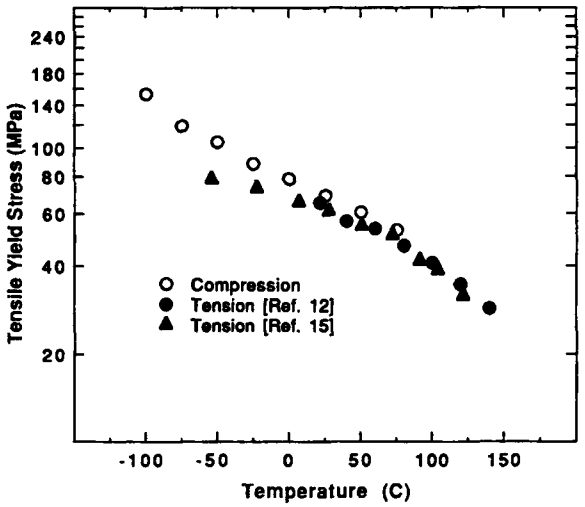

Figure 6 Tensile yield stresses for Lexan®. The open circles were computed from compression data.

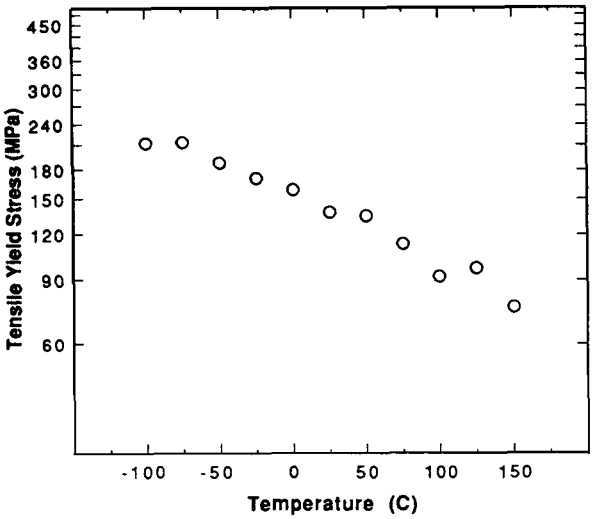

Figure 7 Tensile yield stresses for Ultem®. The open circles were computed from compression data.

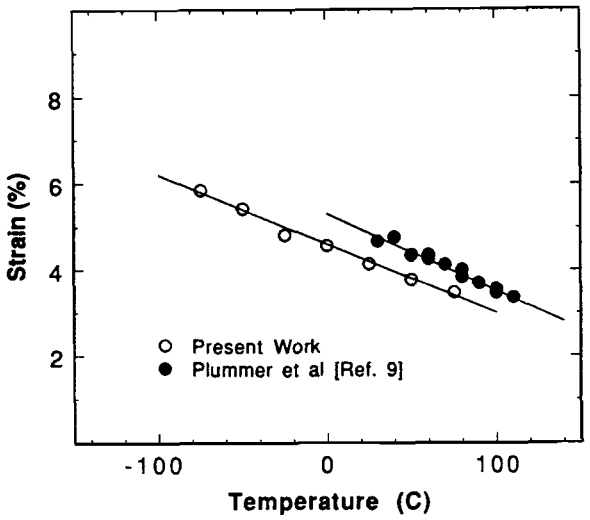

Figure 9 Tensile yield strains for Lexan®. The open circles were computed from the compression yield data using Young's moduli and Poisson's ratio information.

similar, if not identical. From the findings of Plummer and Donald[9] the slight shift in magnitude is expected from the differences in strain rates.

The Effect of Hydrostatic Pressure

A number of reports in the literature[20-24] show that the yield properties of polymer solids are measurably altered by hydrostatic pressure. The usual way that this pressure dependence is expressed[20] is by the addition of a linear correction term to the critical octahedral shear stress in the expression for the Von Mises yield criterion:

$$k_c = k_{co} + \mu P. \tag{2}$$

Here k_c is the critical octahedral shear stress, μ the pressure coefficient, and P the pressure. Using tensile and compression yield data we can obtain values for the pressure coefficients using the expressions developed in Appendix B. These data are shown in Table IV along with collected literature values. Where direct comparisons are possible the values computed from our experiments agree very well with the literature data.

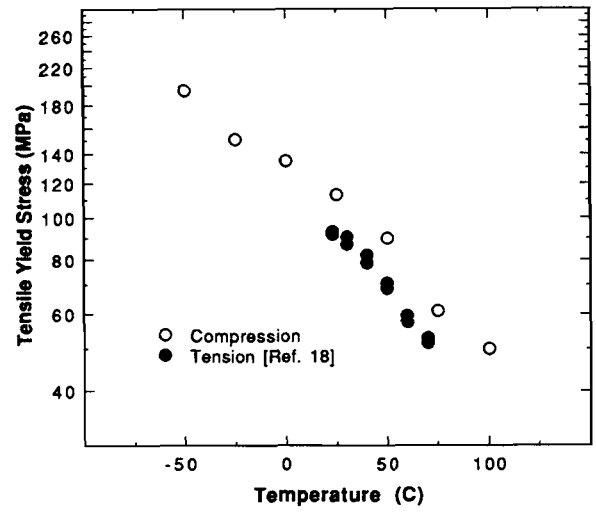

Figure 8 Tensile yield stresses for Zytel® 330. The open circles were computed from compression data.

Table IV Pressure Coefficients of the Yield Stress

Polymer	t (°C)	μ	Ref.
Lexan®	25	0.09	
	50	0.10	
	75	0.10	
	−50 to 200	0.08	21
		0.05	22
		0.07	23
Polyethylene terephthalate	25	0.08	
	50	0.05	
		0.09	20
		0.08	24
Arylon®	25	0.05	
	25	0.06	
Zytel® 330	25	0.26	
	50	0.31	
	75	0.35	

Critical Crazing Stress

Narizawa et al.'s determination of the critical crazing stress[6] involves craze formation in a notched specimen in tension. If a notch with a circular root is put in a specimen and a tensile stress applied (either in a tensile test or a bending action), Hill's slip line theory would predict slip lines as shown by the polyarylate sample in Figure 10. By carefully applying the tensile stress, researchers were able to visually observe the slip lines and the formation of crazes above the notch.[25] In all cases the plane of the crazes was normal to the tensile stress. Our experience was similar. We were never able to control the tension sufficiently to observe the craze formation prior to catastrophic failure but, in most cases, a postmortem examination of the fracture surface clearly revealed the craze and its position with respect to the notch could be determined from photomicrographs. Figure 11 is such a photomicrograph. Here we are examining a fracture surface that is normal to the applied tension. The feature in the top, left hand corner is the surface of the notch. The smooth band running from the bottom, left hand corner to the top, right hand corner (parallel to the bottom of the notch) is the remnant of the craze. The distance from the bottom of the notch to the center of the craze is indicated by the arrow. Hill's slip line theory yields the relationship between the tensile stress normal to the craze plane (σ_1), the critical octahedral shear stress ($2k$), the notch radius (r) and the distance of the craze above the notch (x)

$$\sigma_1 = 2k[1 + \ln (1 + x/r)]. \quad (3)$$

Ishikawa et al.[25] and others feel that it is the hydrostatic or mean stress (σ_m) that is critical to craze formation and it can be computed from the same information (assuming Poisson's ratio of 0.5).

$$\sigma_m = k[1 + 2 \ln (1 + x/r)]. \quad (4)$$

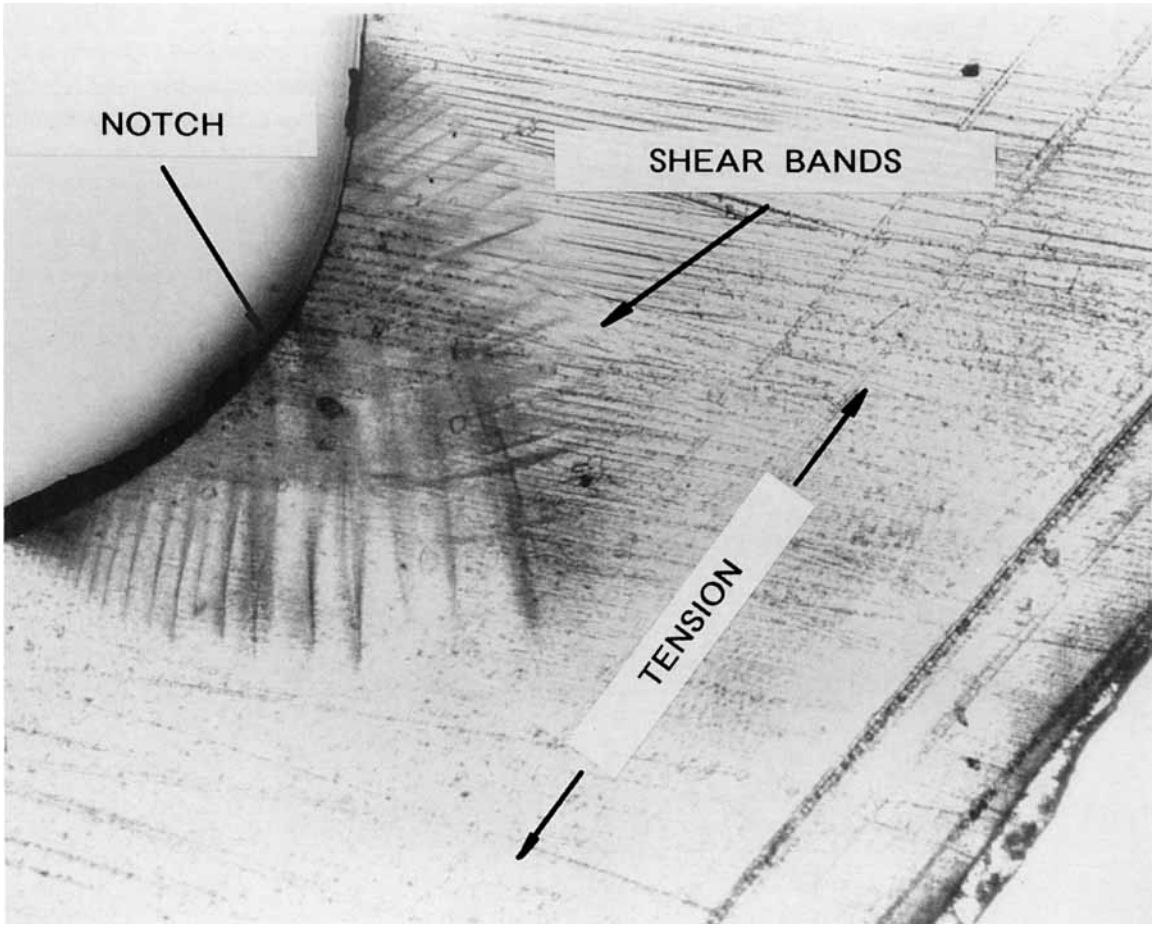

Figure 10 Slip lines. Micrographs taken on sections of notched Arylon® samples strained at room temperature. The notch radius was 0.5 mm.

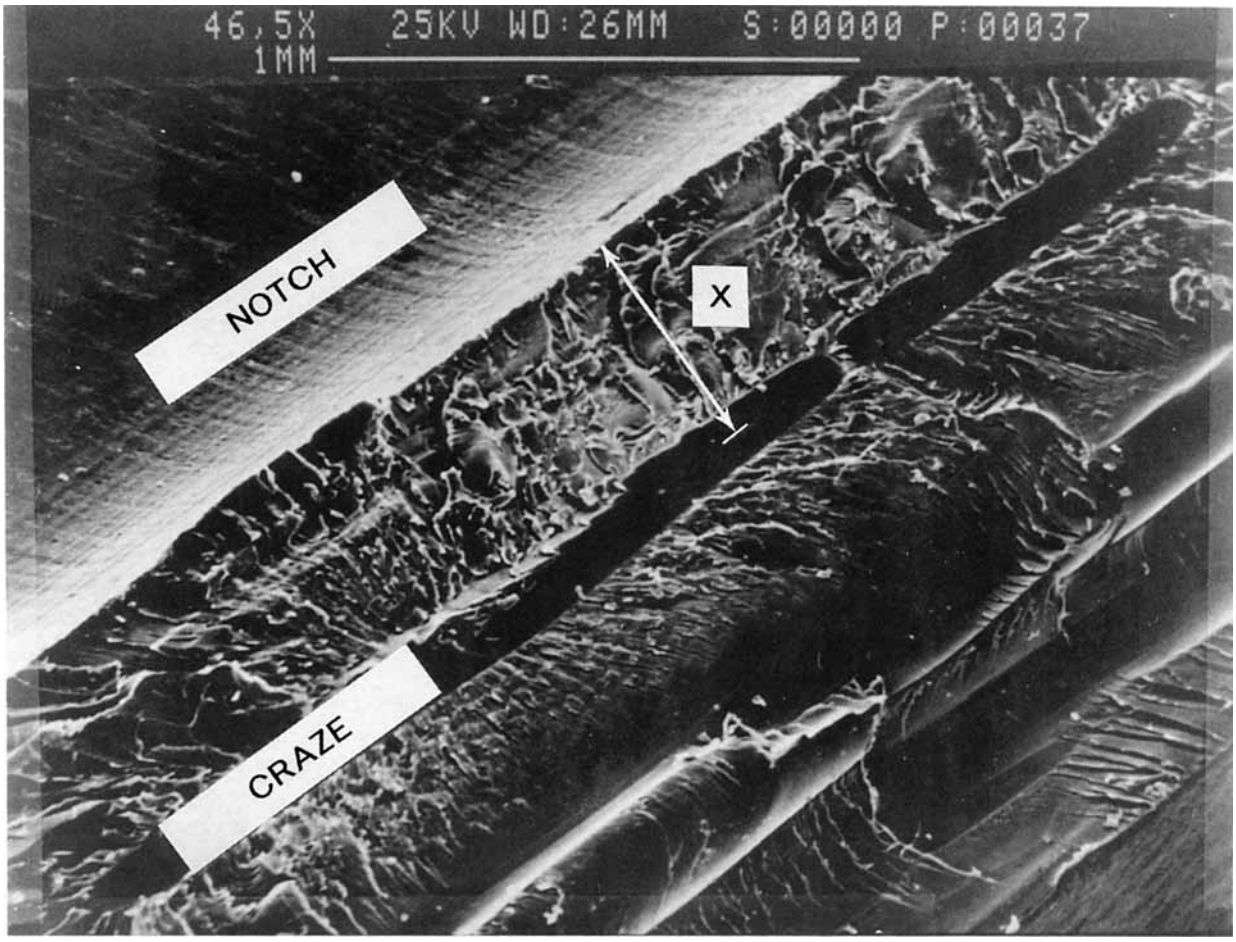

Figure 11 Micrograph of a fractured surface. This is a low magnification, scanning electron micrograph of a fracture surface of Arylon® broken at room temperature. The feature in the top, left hand corner of the micrograph is the notch and the smooth band running from the bottom left hand corner to the top right hand corner of the micrograph is the signature of a craze.

In this study σ_m ranged from slightly more than half of σ_1 to σ_1.

The procedure adopted was to machine notches (0.5 mm radii) into tensile bars at intervals of about 0.75 in. and then anneal the samples as described above. The samples were heated or cooled to the desired temperature and the breaks made in three-point bend while monitoring the load and displacement. As long as the curves had a "saw tooth" appearance, the experiments were continued. If curvature was noted, either thicker specimens were used to obtain a linear load-displacement curve or the measurements were suspended.

The collected data are shown in Figure 12 where the data for the various samples have been shifted for clarity of presentation. The measured ratios of the normal tensile stresses (σ_1) to the octahedral shear stresses ($2k$) are between 1 and 2 with a very slight increase in the ratios as the temperature is increased. The similarity of the data reflect experimental limitations. For easily crazed materials (i.e., polymethylmethacrylate) surface flaws in the notches dominated the fracture process and determinations could not be made. At the other end of the spectrum, plane strain conditions could not be maintained with the sample sizes available and the experiments were suspended.

There is not a great deal of literature data on σ_1 for the polymers studied. Berger[8] has computed the crazing to yield stress ratio for polyarylates and his data are shown in Figure 13. Since his experiments were done in plane stress, comparing with our σ_1 data is proper. The magnitude and trend agree.

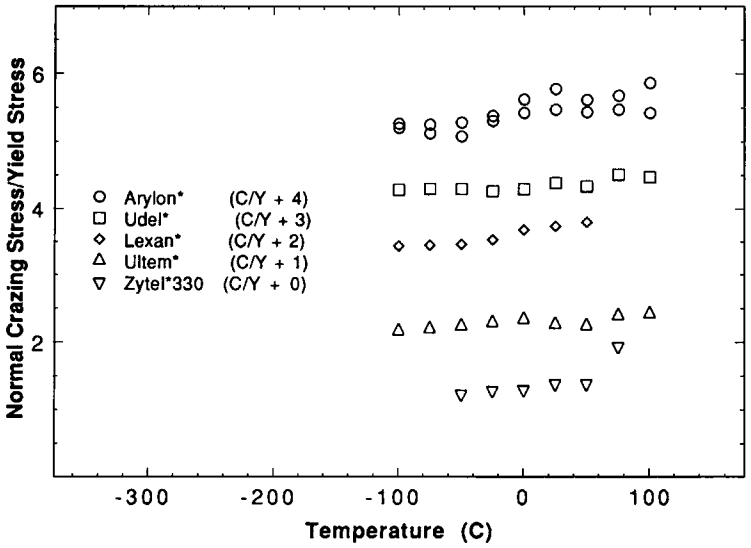

Figure 12 Normal crazing stress/shear yield stress ratios. These data were computed from the position of the crazes with respect to the notches in the fracture surfaces. The data have been shifted vertically for clarity of presentation.

Modulus Determinations

To convert the indentation data to a more familiar form, we faced the task of determining Poisson's ratio. This is easily accomplished if bulk and shear or tensile modulus data are available.[26]

Bulk Moduli

The bulk moduli were determined from pressure–volume information taken in PVT experiments.[27] Pressure–log volume slopes were determined from data collected at pressures ranging from 10–100 MPa.

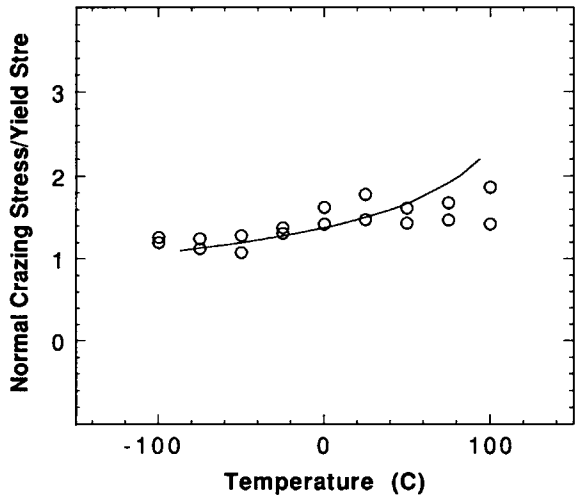

Figure 13 Normal crazing stress/shear yield stress ratios. Circles represent values determined for Arylon® in this work. The line represents data by Berger.[8]

Young's Moduli

The DuPont DMA was used to determine Young's modulus data at 1 Hz.

For the samples studied, in the temperature region between T_g and any major low temperature secondary relaxation, the semilog plots of modulus versus temperature are roughly linear and nearly parallel. Figures 14 and 15 are representative of the data. Table V contains slope and intercept information for the straight line fits. The slopes are given in units of $(1/°C)$ and the intercept information is presented as the moduli at 0°C. You will note the similarity of the slopes for the various pairs of data indicating a constant Poisson's ratio in that region.

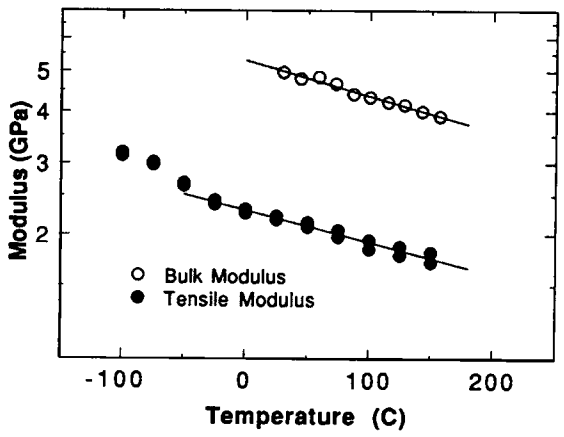

Figure 14 Bulk and tensile modulus data for Arylon®.

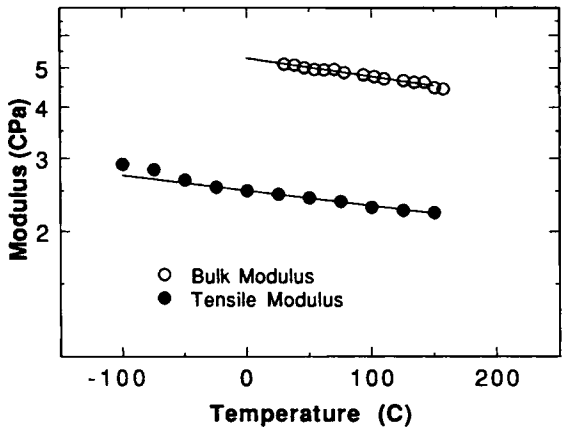

Figure 15 Bulk and tensile modulus data for Udel®.

The variation in the tabulated Poisson's ratios is within the experimental errors.

DISCUSSION

Using the determined triaxial crazing stresses (σ_m) and the bulk moduli we can calculate the volume expansion at craze formation (crazing strains) assuming a linear stress–strain relationship. Similarly we can use our Young's modulus and Poisson's ratio data to compute a shear modulus that we can use with our determined values of the octahedral shear yield stress ($2k$) to compute the shear yield strains. Representative plots of the data are shown in Figures 16 and 17. There is considerable scatter in the σ_m data. To a fair approximation, the data can be represented by the straight lines as shown and tabulated information on such straight line fits are given in Table VI. In each case we present the slope of the lines and the extrapolated value of the stress or strain at T_g.

Table V Poission's Ratio

		−Slope	Intercept	Poisson's Ratio
Arylon®	B	0.0020	5.3	0.43
	E	0.0020	2.3	
Udel®	B	0.0010	5.3	0.42
	E	0.0010	2.6	
Lexan®	B	0.0019	4.6	0.42
	E	0.0019	2.2	
Ultem®	B	0.0016	6.3	0.41
	E	0.0017	3.3	
Zytel® 330	B	0.0018	5.8	0.40
	E	0.0026	3.3	

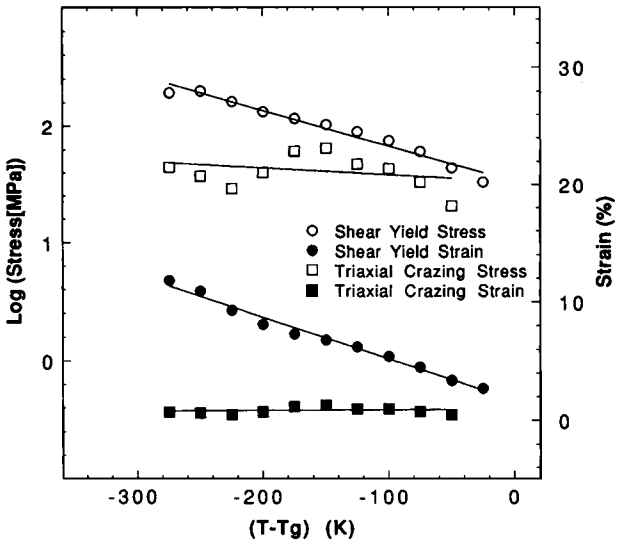

Figure 16 Crazing and yield characterization of Arylon®.

There is similarity among the various polymer glasses examined. The magnitudes and the temperature dependences of the yielding and crazing parameters are similar but not identical. This is seen in Figure 18. The shear yield stresses for the five polymers cluster quite well but measurable differences are noted. The crazing stresses and the shear yielding strains show the same behavior. The triaxial crazing strains in Figure 19 may be different. In this figure we have attempted to let the size of the points reflect the experimental uncertainty in the strain axis. The data for the various polymer samples are indistinguishable. Two other features are noted.

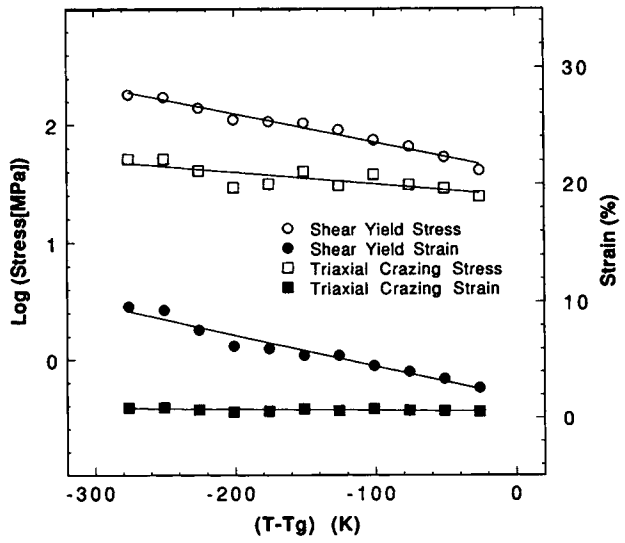

Figure 17 Crazing and yield characterization for Udel®.

Table VI Tabulated Data

	−Slope (°C^{-1})	Stress (T_g) (MPa)	Temp. Range (°C)
Triaxial crazing stress (σ)			
Arylon®	0.0006	34	−100–150
Udel®	0.0010	25	−100–150
Lexan®	0.0006	48	−100–75
Ultem®	0.0001	47	−100–150
Zytel® 330	0.0008	54	−50–100
Shear yield stress ($2k$)			
Arylon®	0.0030	33	−100–150
Udel®	0.0024	40	−100–150
Lexan®	0.0025	41	−100–75
Ultem®	0.0017	79	−100–150
Zytel® 330	0.0036	42	−50–100
	−Slope (%/°C)	**Strain (T_g) (%)**	
Triaxial crazing strain			
Arylon®	−0.0005	0.9	−100–150
Udel®	0.0009	0.6	−100–150
Lexan®	−0.0008	1.4	−100–75
Ultem®	−0.0009	1.0	−100–150
Zytel® 330	−0.0004	1.2	−50–100
Shear yield strain			
Arylon®	0.035	1.7	−100–150
Udel®	0.027	1.8	−100–150
Lexan®	0.032	3.2	−100–75
Ultem®	0.017	4.3	−100–150
Zytel®	0.029	1.7	−50–100

There is very little temperature dependence of the triaxial crazing strains and their magnitudes are small, <1.5%.

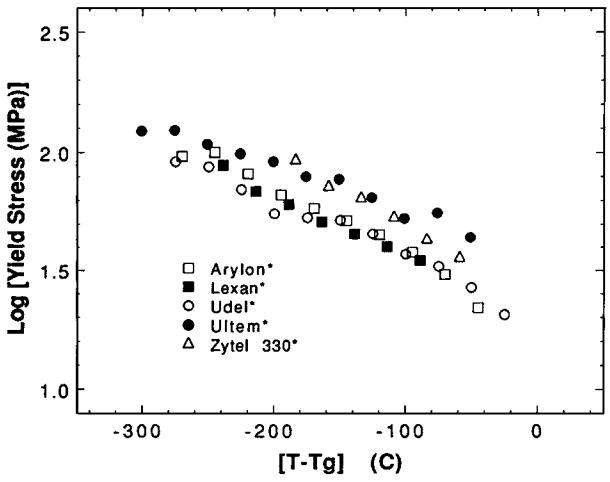

Figure 18 Shear yield stresses normalized to T_g.

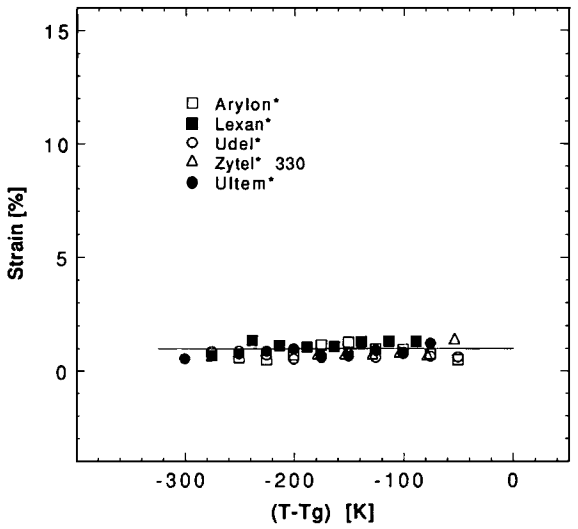

Figure 19 Triaxial crazing strains normalized to T_g.

APPENDIX A

In terms of the principal stresses (σ_1, σ_2, and σ_3) we can write the Von Mises yield criterion as:

$$\sqrt{6}k = \sqrt{(\sigma_1 - \sigma_1)^2 + (\sigma_1 - \sigma_3)^2 + (\sigma_2 - \sigma_3)^2}. \tag{A.1}$$

For a tensile test: $\sigma_1 = Y$, $\sigma_2 = \sigma_3 = 0$ and therefore:

$$\sqrt{3}k = Y. \tag{A.2}$$

For pure shear: $\sigma = \sigma_1 = -\sigma_2$, $\sigma_3 = 0$ and thus:

$$k = \sigma. \tag{A.3}$$

For our compression test: $\sigma_1 = -S$, $\sigma_2 = 0$, $\epsilon_3 = 0$ where ϵ_1, ϵ_2, and ϵ_3 are the principal strains. We can therefore write the generalized Hooke's Law as (ν = Poisson's ratio):

$$\epsilon_1 E_1 = -S - \nu\sigma_3$$

$$\epsilon_2 E_2 = \nu S - \nu\sigma_3$$

$$0 = \nu S + \sigma_3$$

and thus:

$$\sqrt{3}k = S\sqrt{(1 - \nu + \nu^2)}. \tag{A.4}$$

We therefore have relationships between our measured, compressional yield stress (S) and the conventional tensile (Y) or shear (σ) yield stress.

APPENDIX B

The pressure dependence of polymer yield is considered by assuming a Von Mises yield criterion and then adding a linear pressure correction term to the octahedral shear stress (k).[20,21,24]

$$k + k_o + \mu P \tag{B.1}$$

k_o is the pressure independent octahedral shear stress and μP the pressure correction. μ is the pressure coefficient and P the hydrostatic pressure defined:

$$P = (-1/3)[\sigma_1 + \sigma_2 + \sigma_3]. \tag{B.2}$$

If we substitute the above expressions for k and P into the usual relationship for the Von Mises criterion (Appendix A), then we find:

$$k_o = (S/3)[\sqrt{3(1 - \nu + \nu^2)} - \mu(1 + \nu)] \tag{B.3}$$

where ν is Poisson's ratio. The pressure coefficient can be defined in terms of any two yield experiments:

$$\mu = 3(\sigma/Y) - \sqrt{3} \tag{B.4}$$

or

$$\mu = \sqrt{3}\left[\frac{\sqrt{(1 - \nu + \nu^2)} - (Y/S)}{(Y/S) + (1 + \nu)}\right] \tag{B.5}$$

etc. If we define $k_o = k'_o$ when $\mu = 0$, then we can get an idea for the magnitude of the pressure correction.

$$(k_o/k'_o) = 1 - \left[\frac{\mu(1 + \nu)}{\sqrt{3(1 - \nu + \nu^2)}}\right]. \tag{B.6}$$

If we let $\mu = 0.42$ (see Table IV) then

$$(k_o/k'_o) = 1 - 0.9426\mu. \tag{B.7}$$

μ was found to range from 0.03 to ~0.35. Since the uncertainties of the measured yield stresses are usually >5%, the pressure corrections are not warranted in most cases. Zytel® 330 may be an exception.

We acknowledge and sincerely appreciate the comments and help of R. J. Farris (Univ. of Massachusetts), L. L. Berger, D. D. Huang, and D. C. Cooke. We also thank H. W. Starkweather, Jr. and W. G. Kampert for the Young's modulus measurements, D. J. Walsh and B. J. Haley, Jr. for the PVT data, and D. D. Huang and J. C. Coburn for tensile data.

REFERENCES

1. J. G. Williams, *Fracture Mechanics of Polymers,* Ellis Horwood Ltd., Chichester, England, 1984.
2. E. H. Andrews, in *The Physics of Glassy Polymers,* Chap. 7, Applied Science Pub. Ltd., London, 1973.
3. E. J. Kramer and L. L. Berger, *Adv. Polym. Sci.* 91/92, Springer–Verlag, Berlin, 1990.
4. P. B. Bowden, in *The Physics of Glassy Polymers,* Chap. 5, N. Haward, Ed. Applied Science Pub. Ltd., London, 1973.
5. D. E. Walrath and D. F. Adams, Verification and Application of the Iosipescue Shear Test Method, Report #UWME-RD-401-103-1, Dept. of Mechanical Engineering, University of Wyoming, June 1984.
6. I. Narizawa, M. Ishikawa, and H. Ogawa, *Phil. Mag. A,* **41,** 331–351 (1980).
7. K. Cho and A. N. Gent, *J. Matl. Sci.,* **23,** 141–144 (1988).
8. L. L. Berger; private communication.
9. C. J. G. Plummer and A. M. Donald, *J. Poly. Sci., Polymer Phys.,* **27,** 327 (1989).
10. R. P. Kambour; *Polym. Commun.,* **25,** 130–132 (1984).
11. R. Hill, *The Mathematical Theory of Plasticity,* Oxford Univ. Press, Oxford, 1950.
12. M. Ishikawa and I. Narizawa, *J. Matl. Sci.,* **18,** 2826–2834 (1983).
13. C. Bauwens–Crowet, J. C. Bauwens, and G. Homes, *J. Poly. Sci. A-2,* **7,** 735–742 (1969).
14. J. C. Bauwens, C. Bauwens–Crowet, and G. Homes, *J. Poly. Sci. A-2,* **7,** 1745–1754 (1969).
15. J. S. Foot, R. W. Truss, I. M. Ward, and R. A. Duckett, *J. Matl. Sci.,* **22,** 1437–1442 (1987).
16. A. T. DeBenedetto and K. L. Trachte, *J. Appl. Poly. Sci.,* **14,** 2249–2262.
17. J. C. Coburn, private communication.
18. D. D. Huang, private communication.
19. P. B. Bowden and J. A. Jukes, *J. Matl. Sci.,* **7,** 52–63 (1972).
20. C. Bauwens–Crowet, J. C. Bauwens, and G. Homes, *J. Matl. Sci.,* **7,** 176–183 (1972).
21. J. A. Sauer, D. R. Mears, and K. D. Pae, *Eur. Polym.,* **6,** 1015 (1970).
22. A. Christiansen, S. V. Radcliffe, and E. Baer, *Phil. Mag.,* **24,** 451–467 (1971).
23. S. Rabinowitz, I. M. Ward, and J. S. C. Parry, *J. Matl. Sci.,* **5,** 29–39 (1970).
24. M. Ishikawa and I. Narizawa, *J. Matl. Sci.,* **18,** 1947–1957 (1983).
25. M. Ishikawa, I. Narizawa, and H. Ogawa, *J. Poly. Sci., Poly. Phys. Ed.,* **15,** 1791–1804 (1977).
26. T. Alfrey, Jr., *Mechanical Behavior of High Polymers,* Interscience Pub., Inc., New York (1948).
27. P. Zoller, *J. Poly. Sci., Poly. Phys. Ed.,* **16,** 1261–1275 (1978).

Received July 11, 1991
Accepted April 3, 1992